Title: Efficacy of CDK4/6 inhibitors in preclinical models of malignant pleural mesothelioma.

Authors: Elisabet Aliagas,[1] Ania Alay,[1,2] Maria Martínez-Iniesta,[3] Miguel Hernández-Madrigal,[1] David Cordero,[1,2,4] Mireia Gausachs,[1] Eva Pros,[5] Maria Saigí,[5] Sara Busacca,[6] Annabel J. Sharkley,[7] Alan Dawson,[8] Ramón Palmero,[1,9] José C. Ruffinelli,[9] Susana Padrones,[10] Samantha Aso,[10] Ignacio Escobar,[11] Ricard Ramos,[11] Roger Llatjós,[12] August Vidal,[12] Eduard Dorca,[12] Mar Varela,[12] Montse Sánchez-Céspedes,5 Dean Fennell,[6,13] Cristina Muñoz-Pinedo,[1] Alberto Villanueva,[3] Xavi Solé,[1,2,4] and Ernest Nadal[1,9,14]

1. Preclinical and Experimental Research in Thoracic Tumors (PrETT) group. Oncobell Program. Bellvitge Biomedical Research Institute (IDIBELL), L'Hospitalet de Llobregat (Barcelona), Spain
2. Unit of Bioinformatics for Precision Oncology, Catalan Institute of Oncology (ICO), L'Hospitalet de Llobregat (Barcelona), Spain
3. Chemoresistance group. Oncobell Program, Bellvitge Biomedical Research Institute (IDIBELL), L'Hospitalet de Llobregat (Barcelona), Spain
4. Consortium for Biomedical Research in Epidemiology and Public Health (CIBERESP), Barcelona, Spain
5. Cancer Genetics Group, Josep Carreras Leukaemia Research Institute (IJC), Badalona, Barcelona, Spain
6. Department of Genetics and Genome Biology, Leicester Cancer Research Centre, University of Leicester, Leicester, UK
7. University of Sheffield Teaching Hospitals, Sheffield, UK
8. Department of Thoracic Surgery, Glenfield Hospital, Leicester, UK
9. Department of Medical Oncology, Catalan Institute of Oncology, L'Hospitalet de Llobregat (Barcelona), Spain
10. Department of Respiratory Medicine, Hospital Universitari de Bellvitge, L'Hospitalet de Llobregat (Barcelona), Spain
11. Department of Thoracic Surgery, Hospital Universitari de Bellvitge, L'Hospitalet de Llobregat (Barcelona), Spain

[12.] Department of Pathology, Hospital Universitari de Bellvitge, L'Hospitalet de Llobregat (Barcelona), Spain

[13.] Mesothelioma Research Programme, Department of Genetics and Genome Biology, University of Leicester, Leicester, UK

[14.] Department of Clinical Sciences, School of Medicine and Health Sciences, Universitat de Barcelona, Campus Bellvitge, L'Hospitalet del Llobregat (Barcelona), Spain

Correspondence to: Dr. Ernest Nadal. Department of Medical Oncology. Catalan Institute of Oncology. Avda Gran Via 199-203. L'Hospitalet de Llobregat (Barcelona), Spain. Phone: +34 93 260 7744. Email: esnadal@iconcologia.net. ORCID ID: https://orcid.org/0000-0002-9674-5554.

Competing interest: E. Nadal received research support from Roche, Pfizer, Bristol Myerss Squibb and Merck Serono and participated in advisory boards from Bristol Myers Squibb, Merck Serono, Merck Sharpe & Dohme, Lilly, Roche, Pfizer, Takeda, Boehringer Ingelheim, Bayer, Amgen and AstraZeneca. R. Palmero has participated in advisory boards from Bristol Myers Squibb, Merck Sharpe & Dohme, Roche, Pfizer, Lilly, Boehringer Ingelheim and AstraZeneca. D. Fennell has received research support from Astex Therapeutics, Astra Zeneca, Bayer, Boehringer Ingelheim, Bristol Myers Squibb, Clovis Oncology, Merck Sharpe & Dohme, Lilly Oncology, Roche and participated in advisory boards from Atara Therpeutics, Bayer, Boehringer Ingelheim and Inventiva. The other authors do not have conflict of interest to disclose.

Abstract

Background: There is no effective therapy for patients with malignant pleural mesothelioma (MPM) who progressed to platinum-based chemotherapy and immunotherapy.

Methods: We aimed to investigate the antitumor activity of CDK4/6 inhibitors using *in vitro* and *in vivo* preclinical models of MPM.

Results: Based on publicly available transcriptomic data of MPM, patients with *CDK4* or *CDK6* overexpression had shorter overall survival. Treatment with abemaciclib or palbociclib at 100 nM significantly decreased cell proliferation in all cell models. Both CDK4/6 inhibitors significantly induced G1 cell cycle arrest thereby increasing cell senescence and increased the expression of interferon signalling pathway and tumour antigen presentation process in culture models of MPM. *In vivo* preclinical studies showed that palbociclib significantly reduced tumour growth and prolonged overall survival using distinct xenograft models of MPM implanted in athymic mice.

Conclusions: Treatment of MPM with CDK4/6 inhibitors decreased cell proliferation, mainly by promoting cell cycle arrest at G1 and by induction of cell senescence. Our preclinical studies provide evidence for evaluating CDK4/6 inhibitors in the clinic for the treatment of MPM.

Keywords: malignant pleural mesothelioma, CDK4/6 inhibitors, drug therapy, MPM *in vivo* models.

Introduction

Malignant pleural mesothelioma (MPM) is an aggressive, locally invasive and currently not curable malignancy of the pleura, which is associated with occupational and para-occupational exposure to asbestos (1). Although asbestos use is banned in many countries, asbestos-insulated buildings are present throughout the world and some countries are still manufacturing and using large quantities of asbestos (2). Germline mutations in *BAP1* and in other cancer susceptibility genes such as *PALB2, BRCA2, CHEK2* and *MLH1* have been identified in about 10-15% of patients with MPM (3-7).

Treatment options are limited for patients with advanced MPM (8). Cisplatin plus pemetrexed has been the standard treatment in patients with advanced MPM (9). The addition of bevacizumab to chemotherapy modestly improved overall survival, but this treatment is not available in all countries (10). Single agent immunotherapy has demonstrated limited efficacy in the relapsed setting versus chemotherapy in the PROMISE trial, while in the CONFIRM trial nivolumab has been superior to placebo (11, 12). Recently, in the CheckMate-743 study, dual immune checkpoint inhibition with nivolumab plus ipilimumab has demonstrated superiority to platinum plus pemetrexed in the 1st line setting and has been already approved by the FDA (13).

Comprehensive genomic analysis of MPM revealed that is dominated by inactivation of tumour suppressor genes by multiple mechanisms including single nucleotide variants (SNVs), copy number losses, gene fusions and splicing alterations (14, 15). Commonly inactivated tumour suppressor genes include cyclin-dependent kinase inhibitor 2A (*CDKN2A*), BRCA1 associated protein 1 (*BAP1*) and neurofibromin 2 (*NF2*), large tumour suppressor kinase 2 (*LATS2*) and SET Domain Containing 2 (*SETD2*). MPM is characterised by chromosomal instability and extensive somatic copy number alterations with recurrent allelic losses in regions such as 1p, 3p21, 6q, 9p21, 15q11-15 and 22q (16).

CDKN2A deletions are found in 56-70% of MPM and are associated with shorter overall survival (17, 18). The C*DKN2A/ARF* locus (9p21) encodes for two cell cycle regulatory proteins: p14ARF and p16INK4a, the latter being a negative

regulator of cyclin-dependent kinase 4/6 (CDK4/6) (19, 20). In a recent clinical trial of personalised therapy in advanced NSCLC, *CDKN2A* loss was associated with sensitivity to CDK4/6 inhibitors (19, 21). Considering the high frequency of *CDKN2A* deletions in MPM and the fact that cell cycle deregulation is a hallmark of this disease, we postulated that CDK4/6 inhibitors might constitute a novel therapeutic approach in MPM. In the last decade, several selective CDK4/6 inhibitors, abemaciclib, ribociclib and palbociclib, have been approved for the treatment of metastatic breast cancer (22-24).

In the present work, we investigated the efficacy of CDK4/6 inhibitors in preclinical models of MPM to investigate their potential in the treatment of MPM. We also assessed the prognostic impact of *CDK4* or *CDK6* overexpression in primary tumours in patients with MPM using publicly available transcriptomic data.

Materials and methods

Cell culture and cell lines

Five human MPM cell lines, including H28, H2452, H2052, MSTO-211H and H226 were purchased from the American Type Culture Collection (ATCC, Manassas, Virginia). Three additional primary cell lines (ICO_MPM1, ICO_MPM2 and ICO_MPM3) were derived from pleural effusions obtained from three patients with MPM. ICO_MPM1 and ICO_MPM3, were derived from two patients who progressed to standard chemotherapy with platinum and pemetrexed, while ICO_MPM2 was derived from a chemotherapy-naïve patient. Primary cells were isolated and cultured as previously described (25). All cell lines were incubated and maintained at 37˚C in a humidified chamber containing 5% CO_2. All cells were tested routinely (after defrosting or every four months) for mycoplasma contamination by PCR. MSTO-211H and ICO_MPM3 cells were used for the in vivo experiments because they were able to form tumours in athymic mice.

Patient and tissue samples

Patients with confirmed histological diagnosis of malignant pleural mesothelioma were scheduled for routine surgery involving extended pleurectomy decortication at the Glenfield Hospital (University of Leicester). Patients were approached 24 hours prior to their operation and provided with patient information regarding the research. All patients signed informed consent prior to surgery. Seventy-nine patient MPM samples were obtained at the time of surgery. Following surgery, all patients were longitudinally tracked until disease progression with CT monitoring, and monitored for survival.

Oncoscan Analysis

DNA was extracted with the GeneRead DNA FFPE kit (Qiagen, Manchester, UK). Eighty nanograms of genomic DNA were analysed using the OncoScan FFPE Assay Kit (Affymetrix, Wooburn Green High Wycombe, UK). The BioDiscovery Nexus Express 10.0 for OncoScan software was used to determine copy number alterations and loss of heterozygosity (LOH).

Antibodies and drugs

Antibodies against total Rb (#9313), p-Rb (#8180), CDK4 (#12790), CDK6 (#13331), cyclin D1 (#2922), p16 (#80772) and β-actin (#4970) were purchased from Cell Signaling Technology (Danvers, Massachusetts) and were used following manufacturer instructions for western blot.

Abemaciclib (LY2835219) was purchased from Selleckchem (Houston, Texas). Palbociclib (PD0332991) was provided by Pfizer, Inc (San Diego, California). Cisplatin, pemetrexed and gemcitabine were obtained at the Catalan Institute of Oncology pharmacy.

In vitro and *in vivo* drug experiments

For *in vitro* experiments, cell lines were plated into 6-well plates and treated with abemaciclib or palbociclib with 0 (control), 10, 100, 250 or 500 nM for 1, 3 or 15 days. Doses below micromolar range would be clinically well tolerated. For *in vivo* assays, mice were randomly treated with i) vehicle, 200 μl of 0.05 N sodium lactate pH 4.0 by oral gavage five days a week; ii) cisplatin alone, 3.5 mg/kg

administered intraperitoneally once a week or combined with pemetrexed, 100 mg/kg administered intraperitoneally twice a week; iii) gemcitabine, 75 mg/kg administered intraperitoneally twice a week; iv) abemaciclib, 150 mg/kg by oral gavage five days over seven days or v) palbociclib, 150 mg/kg by oral gavage five days over seven days. Mice with subcutaneous tumours were treated during twenty-six days, while mice harbouring orthotopic lung derived MSTO-211H and ICO_MPM3 xenografts were treated during forty days and fifty-two days, respectively.

Western blot analysis

Total cell lysates and western blotting were performed as previously described (26).

Cell viability, cell cycle and apoptosis analysis

Cell viability was evaluated by cell counting and colony formation assays as described elsewhere (27). For colony formation tests cells were grown for 15 days and medium was renewed every 4 days. Cell cycle and apoptosis were analysed by flow cytometry and propidium iodide incorporation as described in (28). A minimum of $1x10^4$ cells were analysed per determination. All experiments were repeated at least three times with similar results: cell counting assay comprised 3 measurements in 3 biological replicates; cell cycle comprised 3 biological replicates; and apoptosis comprised multiple biological replicates 10 for MSTO-211H, 4 for H28 and 3 for ICO_MPM3. P-values were adjusted using FDR.

Measurement of cellular senescence

The evaluation of senescence-associated β-Galactosidase (SA-β-Gal) expression was performed as previously described (29). Experiments included 3 measurements in at least 3 biological replicates.

***In vivo* MPM subcutaneous preclinical drug assays in nude mice**

To investigate the efficacy of palbociclib in the treatment of MPM, we used the MSTO-211H cell line, derived from a patient who had not received prior chemotherapy and able to grow in athymic mice. For subcutaneous xenograft

development, 4 x 10^6 MSTO-211H cells growing exponentially were suspended in 300 μl PBS and subcutaneously inoculated into the right flanks of 23 six-week-old male athymic nude (Hsd:Athymic Nude-Foxn1^{nu}) mice (Envigo, Indiana, Indianapolis). Once the tumours reached a homogeneous average volume size of 300–400 mm^3 as including criteria, mice (n=21) were randomly assigned into three groups (n=7 per group) and treated with i) vehicle; ii) cisplatin combined with pemetrexed or iii) palbociclib as described above. To evaluate efficacy, tumour volumes ($V=\pi/6 \times L \times W^2$) were measured twice per week with callipers and the weight of each animal was measured every day. After 26 days of treatment, mice were euthanised by cervical dislocation and the tumours were excised, weighted and processed for histologic and RNA studies following standard protocols. The mean volume + SD were calculated using R software v.3.5.0 (30). Daily differences among treatments were analysed using Kruskal-Wallis tests, with FDR adjustment.

In vivo MPM orthotopic preclinical drug assays in tumours nude mice

To investigate the efficacy of CDK4/6 inhibitors in tumours after progression to standard first-line chemotherapy, we generated two different chemoresistant MPM orthotopic models by implanting i) MSTO-211H subcutaneous xenografted tumours treated with cisplatin plus pemetrexed from the previous experiments or ii) chemoresistant patient-derived subcutaneous xenografted tumours in the thoracic cavity of six-week-old male athymic nude mice following our previously reported procedures (31). As we described, mice were anesthetised with a continuous flow of 1% to 3% isoflurane/oxygen mixture (2 L/min) and subjected to right thoracotomy. Mice were situated in left lateral decubitus position, and a small transverse skin incision (5–8 mm) was made in the right chest wall. Chest muscles were separated by a sharp dissection and costal and intercostal muscles were exposed. An intercostal incision of 2 to 4 mm on the third or fourth rib on the chest wall was made and a small tumour piece of 2 to 4 mm^3 was introduced into the chest cavity and the tumour specimens were anchored to the lung surface with Prolene 7.0 suture. Next, the chest wall incision was closed with surgery staples, and finally chest muscles and skin were closed. The waiting time between tumour implantation and the beginning of treatments was of 2 weeks

based on our previous orthotopic xenograft MPM models experience. For the orthotopic xenograft model, thirty-three mice were randomised into three groups (n=11 per group) and treated with i) vehicle; ii) cisplatin alone or iii) palbociclib as previously mentioned for forty days. For the patient-derived orthotopic xenograft model, thirty-one mice were randomised into four groups (n=7-8 per group) and treated with i) vehicle; ii) gemcitabine; iii) abemaciclib or iv) palbociclib as previously described for fifty-two days. In both orthotopic experiments, mice were weighed daily and monitored for the presence of breathing problems. After stopping treatments, all live mice remained untreated until human endpoint (defined as presenting respiratory problems or excessive body weight loss). Orthotopic tumours were collected from euthanised mice and processed for histological studies. Survival curves for each cohort of mice were calculated using the Kaplan-Meier method and the differences between groups were compared using Cox proportional hazards model.

Inmunohistochemistry studies

Paraffin sections of subcutaneous MSTO-211H xenografted tumours harvested when the mice were euthanised 26 days post-treatment were used to assess macrophages and NK cells infiltration by immunohistochemistry. Antibodies used were anti-F4/80 (#70076 from Cell Signalling Technologies) as macrophage marker and recombinant anti-NCR1 (ab233558 from Abcam, Cambridge, UK) as NK cell marker. All slides were coded and examined in blinded manner.

***In silico* analysis of publicly available RNA-sequencing data**

Public data from RNA-seq cohorts published by Bueno et al. (14, 15) and The Cancer Genome Atlas (TCGA-MESO) (15) were used to assess differences in survival. Gene expression (log_2(TPM)) was stratified using the median, and Cox proportional-hazards models adjusted for sex, stage, age and histology were fitted to assess differences in survival using R software (30).

Whole Exome Sequencing (WES) and RNA sequencing (RNA-seq) analysis of patient-derived cell lines

Paired-end RNA sequencing was performed on an Illumina HiSeq 2500, with 100 bp long reads. Genomic DNA and total RNA were submitted to the Centro National de Análisis Genómico (CNAG, Barcelona, Spain), for WES and RNA-Seq library preparation and sequencing. All statistical analyses were done using R software v.3.5.0 (30). Sequence data has been deposited at the European Genome-phenome Archive (EGA), which is hosted by the EBI and the CRG, under accession number EGAS00001005352.

Statistics

Cell proliferation assay was assessed using Wilcoxon signed rank tests comparing each treatment with vehicle condition and adjusted using FDR correction. Differences among treatment and vehicle conditions in the cell death experiment were evaluated using Mann-Whitney U test for each comparison and Kruskal-Wallis test if 3 conditions were simultaneously tested and adjusted afterward using FDR. Cell cycle and senescence experiments were analysed using proportion tests taking into consideration all the cells counted in the abovementioned experiments. P-values were adjusted using FDR. For *in vivo* experiments, the analysis of differences in body weight for orthotopic xenografts was computed using a Mann-Whitney U test comparing the first and last day of treatment in each treatment and adjusted with FDR. For subcutaneous xenografts, a longitudinal analysis testing for differences in treatment slopes was done using analysis of covariance. All tests were two-sided, and assumptions were verified for all tests that required it. Homoscedasticity was also verified using a Levene test. Regarding survival analysis, sample size was not calculated since we used publicly available data Bueno et al. (14) and The Cancer Genome Atlas (15). Cox proportional-hazards models adjusted for sex, stage, age, and histology were fitted to assess the differences between gene expression (categorised using the median log2TPM value for each gene). For *in vivo* experiments, a Cox proportional-hazards model was fitted to assess differences among groups. Survival curves were plotted using Kaplan-Meier curves. P-value smaller than 0.05 was considered statistically significant. All statistical analyses were done using R software v.3.5.0 (30).

For additional information about methodology see supplementary material.

Results

Genomic characterization of patient-derived MPM models and baseline expression of genes involved in cell cycle in MPM cell lines

Clinicopathological characteristics and main genomic alterations are shown in **Table 1.** In all three patient-derived cell lines, *CDKN2A/p16* was deleted and *NF2* was wild type, while *BAP1* was mutated in ICO_MPM1 (p.K651Yfs*1) and ICO_MPM2 (p.R60X). Additional information about their mutational profile is provided in **Supplementary Table S1**.

We examined by Western blot the expression levels of CDK4, CDK6, cyclin D1, CDKN2A/p16 and RB proteins in 5 commercial and in 3 patient-derived MPM cell lines (**Figure 1A**). p16 expression was not detected in any cell line, while all cell lines showed some degree of cyclin D1 expression and retained RB expression. CDK4 was expressed at relatively high level in most MPM cells, whereas CDK6 expression appeared to be comparatively lower. Additional information about their mutational profile is provided in **Supplementary Table S2.**

Antiproliferative effect of CDK4/6 inhibitors on human MPM cell lines

All MPM cell lines treated with increasing concentrations of abemaciclib or palbociclib for 72 hours, showed a decrease in cell number (**Figure 1B and Supplementary Figure S1).** Treatment with abemaciclib and palbociclib at 100 or 500 nM significantly reduced cell number in comparison to control in all cell lines tested ($p<0.05$). At 10 nM, the cell number was significantly reduced in six out of eight cell lines after treatment with abemaciclib ($p<0.01$), while it was significantly reduced in all cell lines after palbociclib treatment ($p<0.05$).

The reduction in cell number after exposure to CDK4/6 inhibitors at 100 nM was nearly 50% (mean 54.5% ± 5.5 with abemaciclib and mean 53.4% ± 4.9 with palbociclib). At 500 nM, a reduction of 64.3% and 64.1% was observed with abemaciclib and palbociclib respectively. MSTO-211H was the most sensitive cell line to both CDK4/6 inhibitors at 100 nM and 500 nM doses. All primary cell lines

were sensitive to CDK4/6 inhibitors regardless of whether they had been derived from a patient who was chemotherapy-naïve or who had received prior chemotherapy. ICO_MPM2, which was derived from a chemotherapy-naïve patient, was the most sensitive primary cell line to palbociclib with a cell number reduction of 45.3% ± 5.2 at 100 nM (**Figure 1B**). These antiproliferative effects were confirmed by cell colony formation assay and crystal violet staining (**Supplementary Figure S2A**). The ability to form colonies was completely blocked when H226, H2052, ICO_MPM1 and ICO_MPM3 were treated with abemaciclib and palbociclib at 250 and 500 nM **(Figure 1C)**.

Effect of CDK4/6 inhibitors on cell cycle in human MPM cell lines

Three cell lines selected for expressing high levels of CDK4 and CDK6 proteins (MSTO-211H, H28 and ICO_MPM3) were evaluated for alterations in cell cycle progression after 24-hour treatment with 250 or 500 nM abemaciclib or palbociclib. Compared with control, all cells treated with abemaciclib or palbociclib at 500 nM were arrested at G1 phase ($p<0.001$, **Figure 2A**). In addition, a significant decrease in cell percentage in the G2/M phase ($p<0.001$) and in S phase ($p<0.001$) was observed in the three cell lines after treatments at 250 nM and 500 nM compared to non-treated cells (**Supplementary Figure S2B**). All changes in the percentage of cells in each phase of the cell cycle after abemaciclib and palbociclib treatment are summarised in **Figure 2B**.

Effect of CDK4/6 inhibitors on cell death and senescence in human MPM cell lines

As a next step, we investigated whether treatment with CDK4/6 inhibitors could induce cell death in MPM cells. MSTO-211H, H28 and ICO_MPM3 cells were treated with different concentrations of abemaciclib and palbociclib, as single agents or in combination with the apoptosis inhibitor QVD for 72 hours and cell death was quantified by FACS (**Supplementary Figure S3**). Neither inhibitor was able to significantly increase the levels of apoptosis in MSTO-211H, H28 and ICO_MPM3 cells at any of the doses tested. At the highest dose (500 nM), the

percentage of apoptotic cells reached 12% with abemaciclib and 8% with palbociclib in MSTO-211H cells, 2% after abemaciclib and 3% after palbociclib in H28 cells, and around 6% after either treatment in ICO_MPM3 cells.

To investigate whether CDK4/6 inhibitors promote senescence, both treated and control MSTO-211H, H28 and ICO_MPM2 cells were stained using β-galactosidase. A significant increase in the percentage of senescent cells was detected in all cell lines treated with different concentrations of abemaciclib or palbociclib ($p<0.001$, **Figure 2C**). Specifically, the proportion of senescent SA-β-gal positive MSTO-211H cells increased from 18% to 54% with 250 nM abemaciclib and to 61% with 500 nM abemaciclib and to 52% with 250 nM palbociclib and to 59% with 500 nM palbociclib. Likewise, an increase of senescent cells was also observed in H28 cells treated with 250 nM or 500 nM of either inhibitor. In ICO_MPM2 cells, the percentage of SA-β-gal positive cells increased from 12% in control cells to 41% after abemaciclib and to 46% after palbociclib treatments at 250 and 500 nM, respectively.

Palbociclib reduced tumour growth and improved overall survival in mice bearing MPM tumours

The effect of palbociclib *in vivo* was examined by implanting subcutaneously MSTO-211H cells into the right flanks of athymic mice. After 26 days of treatment, the mean volume of tumours implanted subcutaneously in vehicle-treated mice was 1816 ± 795.2 mm^3; in cisplatin plus pemetrexed-treated mice was 1647.1 ± 733.8 mm^3 whereas for palbociclib-treated mice it was 524.2 ± 236.6 mm^3 (**Figure 3A and Supplementary Figure S4A**). Differences among palbociclib and the two other cohorts were already statistically significant at day 16 ($p=0.043$, **Figure 3B**). At mice sacrifice, 26 days post-treatment, a significant decrease in the tumour weight was observed for palbociclib-treated mice respect to vehicle and combined chemotherapy-treated mice (0.35 vs 1.1 and 1.13 gr; $p=0.01$ and $p=0.007$, respectively, **Figure 3C and 3D**). No differences were observed at histological level **(Supplementary Figure S5)**. The body weight of the mice was monitored to evaluate the potential side effects of treatments (**Figure 3E**). In those mice treated with palbociclib, no body weight loss was observed during the

experiment, suggesting that palbociclib did not exert significant systemic toxicity at the doses used in this study. After 26 days of treatment, we quantified the macrophages and NK cells infiltration into the subcutaneous MPM tumours xenografts (**Figure 3F**). A statistically significant increase in the tumour associated macrophages ($F4/80^+$ cells) was observed for palbocilicb-treated tumours respect to vehicle and combined chemotherapy-treated tumours (0.09 vs 0.048 and 0.048; p=0.041, respectively, **Figure 3G**). No significant differences in the percentage of tumour infiltrated NK cells ($NCR1^+$ cells) were found between vehicle, cisplatin plus pemetrexed and palbociclib-treated tumours (0.04 vs 0.004 and 0.10; p=0.58, respectively, **Figure 3J**).

To preclinically investigate the efficacy of palbociclib as second-line treatment in MPM tumours refractory to conventional chemotherapy, we re-implanted orthotopically in the thoracic space small fragments from one of the subcutaneous tumours derived from MSTO-211H cells previously treated with cisplatin plus pemetrexed. After 40 days of treatment, no vehicle-treated mice were alive (0/11; 0%); only three platinum-treated mice were alive (3/11; 27.3%), while seven palbociclib-treated mice were still alive (7/11; 63.6%) (**Figure 4A**). Animals (93.9%) were sacrificed due to dyspnoea or excessive weight loss (31/33). Overall survival analysis showed a significant reduction in the risk of death for palbociclib-treated mice compared with vehicle (HR=0.04 [95% CI 0.01-0.17]) or with cisplatin (HR=0.11 [95% CI 0.03-0.41]).

Those mice that were alive after 40 days of treatment (n=10) were maintained without treatment and followed up until endpoint. After six days of stopping treatments, all the remaining platinum-treated mice (n=3) were dead, whereas two out of seven palbociclib-treated mice were still alive after two months without receiving any treatment. Palbociclib treatment did not exert any substantial change in body weight between the first and the last day of treatment **(Supplementary Figure S4B)**. Representative pictures of MSTO-211H orthotopic tumours from each group of treatment are shown in **Figure 4B and Supplementary Figure S6**. Histopathological analysis of the MPM tumour xenografts grown orthotopically in mice accurately reproduced the natural history of mesothelioma **(Figure 4C and Supplementary Figure S7)**.

Next, we generated an additional orthotopic model by implanting into the pleural space of nude mice small tumour fragments harvested from a xenograft generated by injecting subcutaneously the patient derived cell-line ICO_MPM3. Orthotopically implanted mice (n=31) were allocated in the different treatment groups and treatment was started 15 days after implantation, and mice were treated continuously for 52 days. Then, mice were maintained alive without treatment and followed up until human endpoint. (**Figure 4D**). Overall survival analysis shows a significant reduction in the risk of death for palbociclib-treated mice compared with vehicle group (HR=0.23 [95% CI 0.06-0.85]; p=0.027). No significant differences were observed in the risk of death for gemcitabine-treated mice (HR=0.50 [95% CI 0.17-1.40]; p=0.19) and abemaciclib-treated mice (HR=0.42 [95% CI 0.14-1.23]; p=0.12) compared to vehicle. Representative images of orthotopic tumours from each treatment group are shown in **Figure 4E-F**.

Gene-expression profiling in cell lines and xenografts treated with CDK4/6 inhibitors

To determine the functional consequences of CDK4/6 inhibitor treatment, we performed transcriptomic analysis of MSTO-211H cells treated with abemaciclib or palbociclib at 250 nM for 72 hours. In addition, tumour xenografts treated with palbociclib were also evaluated. After treatment with either CDK4/6 inhibitor, a significant downregulation in the expression levels was observed in the MSTO-211H cell line for genes related with cell cycle, such as regulation of transcription genes involved in G1-S transition of mitotic cell cycle, nucleus organization and mitotic spindle assembly and organization (**Supplementary Figure S8 and Supplementary Table S3**). On the other hand, there was a significant upregulation of genes related to interferon signalling pathways, lymphocyte migration and chemotaxis, complement activation and antigen presentation pathways, such as MHC protein complex. Furthermore, the transcriptomic analysis of palbociclib-treated tumours in xenografted mice showed similar results (**Supplementary Figure S9**).

CDK4 and *CDK6* overexpression are associated with poor prognosis in patients with MPM

Based on these results, we evaluated the prognostic value of *CDK4* and *CDK6* overexpression using publicly available transcriptomic data from two cohorts of MPM patients. Patients with *CDK4* overexpression (i.e., above the median) had significantly shorter overall survival in both cohorts (12.6 and 13.3 months, respectively) compared with patients with lower expression (23.5 and 25.9 months respectively). *CDK4* overexpression remained statistically significant after adjusting by age, gender, tumour stage and histologic subtype in each dataset, as well as in the combined analysis of both series (HR=2.10 [95% CI 1.53–2.88]; p=4.2e-06; **Figure 5A**). Patients with *CDK6* overexpression (i.e., above the median) had significantly shorter overall survival (12.6 months) compared with patients with lower expression (20.3 months; p=0.00026) in the Bueno cohort and there was a trend toward shorter overall survival in the TCGA dataset (15 versus 23.6 months; p=0.060). Nevertheless, *CDK6* overexpression remained statistically significant in the combined analysis after adjusting by age, gender, tumour stage and histologic subtype in the Bueno cohort, and also in the combined cohort (HR=1.74 [95% CI 1.32–2.29]; p=5.4e-05; **Figure 5B**).

As previously reported (9,10), low expression of *CDKN2A* was associated with shorter overall survival in both cohorts and was independently associated with worse prognosis in the combined cohort including Bueno and TCGA (HR=0.49 [95% CI 0.36–0.66]; p=3.4e-06; **Supplementary Figure S10A**). In the TCGA cohort, only two tumours harboured an *RB1* homologous deletion, while *CDKN2A/p16* deletion was a common event present in 34 out of 74 cases (46%).

CDKN2A copy number was assessed in an independent cohort of 79 MPM acquired at radical surgery involving extended pleurectomy decortication. Patient clinicopathological characteristics are outlined in **Supplementary Table S4**. Homozygous loss of 9p21.3 encompassing *CDKN2A* was observed in 40 samples (50.6%), while copy number loss/LOH was observed in 18 (22.7%). *CDKN2A* homozygous loss was associated with shorter median overall survival (10.98 months) compared to euploid *CDKN2A* (45.8 months; HR=0.37 [95% CI 0.22 - 0.62]; p=0.0002; **Supplementary Figure S10B**). *CDKN2A* copy number loss/LOH was associated with shorter median overall survival (8.52 months)

compared to wild-type *CDKN2A* (45.8 months; HR=0.18 [95% CI 0.08-0.40]; p=0.0001). There were no statistically significant differences in overall survival among patients harbouring *CDKN2A* homozygous deletion compared to those with *CDKN2A* copy number loss/LOH (HR=0.89 [95% CI 0.49-1.59]; p=0.158).

Discussion

MPM is a rapidly fatal neoplastic disease in which therapeutic options are limited. We investigated the role of CDK4/6 inhibition in MPM because cell cycle deregulation is a relevant hallmark in this disease and *CDKN2A/p16* deletion is a common genomic event associated to worse clinical outcome in MPM (17, 18).

The efficacy of palbociclib has been previously studied in *in vitro* models of MPM (29). However, the antitumour activity of CDK4/6 inhibitors has not yet been evaluated using primary patient-derived cell models of MPM neither *in vivo* models of MPM. In our work, we assessed the efficacy of two CDK4/6 inhibitors, abemaciclib and palbociclib, in a subset of five commercial and three primary patient-derived cell culture models obtained from pleural effusions of patients with MPM (one chemotherapy-naïve and two after progression to standard first-line chemotherapy). Furthermore, we performed not only *in vivo* basic subcutaneous drug response studies in xenografts derived from one chemotherapy-naïve MPM cell line, but also advanced studies by means of orthotopic implanted xenografts from a cell line-derived tumour previously treated with cisplatin plus pemetrexed and from a chemoresistant primary cell line-derived tumour. Remarkably all the cell lines were sensitive to palbociclib and to abemaciclib. Treatment with abemaciclib or palbociclib significantly reduced cell proliferation, as evaluated by cell number counting or by colony formation ability, in all the cell lines including in the primary ones derived from pleural liquid from patients resistant to chemotherapy. *In vitro* experiments underscore two important points: i) no substantial differences were found in the antiproliferative effect of both inhibitors; and ii) the sensitivity to CDK4/6 inhibitors was not correlated with the endogenous expression levels of CDK4 or CDK6. We consider that there is still an unmet need of biomarkers able to predict clinical benefit to CDK4/6 inhibitors. In our work, we

confirmed that *CDKN2A/p16* deletion is associated with shorter overall survival in a cohort of MPM patients with resectable disease. These results are consistent with previous publications where *CDKN2A/p16* loss predicted worse clinical outcome in patients with resected and advanced epithelioid MPM (18).

By analysing publicly available transcriptomic data of MPM, we found that overexpression of CDK4 or CDK6 is also associated with shorter overall survival. Together these findings suggest that cell cycle deregulation may confer an aggressive biological behaviour in mesothelioma and reinforce our hypothesis about further investigating CDK4/6 inhibitors in MPM patients.

We investigated the impact of abemaciclib and palbociclib treatment on cell cycle progression, cellular senescence and apoptosis induction. These experiments were performed using three cell lines that were sensitive to both drugs, including a primary cell line derived from a patient resistant to chemotherapy. As expected, the treatment with abemaciclib and palbociclib caused cell cycle arrest at G1 phase but also promoted cellular senescence. However, neither abemaciclib nor palbociclib activated programmed cell death or apoptosis as indicated by negligible subG1 accumulation or propidium iodide incorporation. The observed increase on cellular senescence induced by both drugs could be linked to apoptosis resistance mechanisms (23, 32). As proposed by other groups (29, 33, 34), our results reinforce the cytostatic mechanism of action of CDK4/6 inhibitors and underscore that these should be given sequentially after completing chemotherapy treatment (35). However, the low cell death observed *in vitro* does not eliminate the possibility that palbociclib, by inducing senescence in a few cells, may promote *in vivo* cytotoxicity mediated by Natural Killer cells. This phenomenon has been described in lung cancer, in which Natural Killers participate in tumour reduction upon treatment with MEK inhibitors and palbociclib (36, 37).

To explore potential activation of compensatory pathways, we performed gene set enrichment analysis of the transcriptome of MSTO-211H cells treated with abemaciclib or palbociclib *in vitro* or subcutaneously implanted in mice. This experiment showed downregulation of genes involved in G1-S transition of mitotic cell cycle, nucleus organization and mitotic spindle assembly and organization.

In concordance with studies conducted in other tumour types, genes encoding interferon signalling and antigen presentation pathways were upregulated after CDK4/6 pharmacological inhibition (34). In melanoma, CDK4/6 inhibition activates p53 by lowering PRMT5 which leads to altered MDM4 splicing and significantly reduced protein expression (38, 39). Other studies performed in breast cancer cell lines and transgenic mice models have shown that abemaciclib treatment increased the expression of antigen processing and presentation and even suppressed the proliferation of regulatory T cells (24, 34). In the present study, we have observed that palbociclib treatment increase the number of tumour associated macrophages in subcutaneous MPM tumour xenografts and there was a trend toward higher NK cell infiltration, but further studies evaluating the functional consequences of the treatment with CDK4/6 inhibitors on the tumour immune contexture are warranted in mesothelioma.

To the best of our knowledge, this is the first time that effectiveness of abemaciclib and palbociclib were evaluated using preclinical *in vivo* subcutaneous and orthotopic MPM tumour models. Among the available cell line models, MSTO-211H cell line was selected for the *in vivo* subcutaneous and orthotopic experiments because i) it expresses CDK4 and CDK6; ii) it is the most sensitive cell line to palbociclib at 500 nM; and iii) it was tumorigenic in athymic mice. Our results showed that palbociclib reduced tumour size in a subcutaneous mouse model of chemo-naïve MSTO-211H cells compared with standard chemotherapy (cisplatin plus pemetrexed). An increased expression of anti-apoptotic proteins after long-term chemotherapy treatment could explain the chemoresistance in this model (40). We tried to replicate a situation representing treatment after progression to platinum-based chemotherapy by generating an orthotopic tumour mouse model and implanting in the pleura small solid fragments of MSTO-211H xenografted tumours previously treated with chemotherapy. In this advanced model of MPM, palbociclib significantly increased the overall survival of mice compared with cisplatin-based chemotherapy or vehicle; the benefits from treatment persisted even after stopping the treatment. Our results reinforce the potential use of palbociclib as a second-line treatment for patients with MPM that is resistant or has relapsed after

standard chemotherapy doublet treatment. Finally, we also use ICO_MPM3, a patient-derived cell line also tumorigenic in athymic mice to test the efficacy of CDK4/6 inhibitors *in vivo*.

Some limitations of our study are the absence of a wide range of available commercial MPM cell lines and the need for preclinical *in vivo* models representing the heterogeneity of the disease, including the adaptive immune system. However, in our study we have combined commercial, primary patient-derived lines as well as orthotopic models where mesothelioma grows in its corresponding microenvironment and can recapitulate the disease behaviour.

A phase II clinical study of abemaciclib in patients harbouring p16ink4a deficient, relapsed MPM has recently completed accrual (NCT03654833). CDK4/6 inhibition in this cohort has been associated radiological responses however the underlying molecular correlates of response are under investigation. Accordingly, whole exome sequencing of the trial cohort is planned to uncover genomic determinants of response.

In conclusion, our data support that treatment with CDK4/6 inhibitors, abemaciclib or palbociclib, can reduce cell proliferation and induce cellular senescence in MPM cell lines and palbociclib can increase overall survival of mice with orthotopically implanted MPM cells. A remarkable and sustained response to palbociclib was observed in xenografts of MPM tumour resistant to cisplatin and pemetrexed which was then implanted orthotopically in the pleural space of mice. Transcriptomic analysis of cell lines and xenografted tumours treated with CDK4/6 inhibitors showed an increased expression of interferon signalling pathway and antigen presenting processes, suggesting that CDK4/6 inhibitors may favour potential response to immunotherapy. Our results warrant further evaluation of CDK4/6 inhibitors as a second-line treatment in patients with advanced MPM that has failed standard platinum-based chemotherapy.

Supplementary information is available at the British Journal of Cancer's website.

References:

1. Delgermaa V, Takahashi K, Park EK, Le GV, Hara T, Sorahan T. Global

mesothelioma deaths reported to the World Health Organization between 1994 and 2008. Bull World Health Organ. 2011;89(10):716-24, 24A-24C.

2. Chen T, Sun XM, Wu L. High Time for Complete Ban on Asbestos Use in Developing Countries. JAMA Oncol. 2019;5(6):779-80.

3. Hassan R, Morrow B, Thomas A, Walsh T, Lee MK, Gulsuner S, et al. Inherited predisposition to malignant mesothelioma and overall survival following platinum chemotherapy. Proc Natl Acad Sci U S A. 2019;116(18):9008-13.

4. Panou V, Gadiraju M, Wolin A, Weipert CM, Skarda E, Husain AN, et al. Frequency of Germline Mutations in Cancer Susceptibility Genes in Malignant Mesothelioma. J Clin Oncol. 2018;36(28):2863-71.

5. Testa JR, Cheung M, Pei J, Below JE, Tan Y, Sementino E, et al. Germline BAP1 mutations predispose to malignant mesothelioma. Nat Genet. 2011;43(10):1022-5.

6. Guo R, DuBoff M, Jayakumaran G, Kris MG, Ladanyi M, Robson ME, et al. Novel Germline Mutations in DNA Damage Repair in Patients with Malignant Pleural Mesotheliomas. J Thorac Oncol. 2020;15(4):655-60.

7. Zauderer MG, Jayakumaran G, DuBoff M, Zhang L, Francis JH, Abramson DH, et al. Prevalence and Preliminary Validation of Screening Criteria to Identify Carriers of Germline BAP1 Mutations. J Thorac Oncol. 2019;14(11):1989-94.

8. Woolhouse I, Bishop L, Darlison L, de Fonseka D, Edey A, Edwards J, et al. BTS guideline for the investigation and management of malignant pleural mesothelioma. BMJ Open Respir Res. 2018;5(1):e000266.

9. Vogelzang NJ, Rusthoven JJ, Symanowski J, Denham C, Kaukel E, Ruffie P, et al. Phase III study of pemetrexed in combination with cisplatin versus cisplatin alone in patients with malignant pleural mesothelioma. J Clin Oncol. 2003;21(14):2636-44.

10. Zalcman G, Mazieres J, Margery J, Greillier L, Audigier-Valette C, Moro-Sibilot D, et al. Bevacizumab for newly diagnosed pleural mesothelioma in the Mesothelioma Avastin Cisplatin Pemetrexed Study (MAPS): a randomised,

633 controlled, open-label, phase 3 trial. Lancet. 2016;387(10026):1405-14.

634 11. Popat S, Curioni-Fontecedro A, Dafni U, Shah R, O'Brien M, Pope A, et al.
635 A multicentre randomised phase III trial comparing pembrolizumab versus single-
636 agent chemotherapy for advanced pre-treated malignant pleural mesothelioma:
637 the European Thoracic Oncology Platform (ETOP 9-15) PROMISE-meso trial.
638 Ann Oncol. 2020;31(12):1734-45.

639 12. Fennel D O, Califano R. Nivolumab versus placebo in relapsed malignant
640 mesothelioma: preliminary results from the CONFIRM phase 3 trial. Presented
641 at: International Association for the Study of Lung Cancer 2020 World Conference
642 on Lung Cancer_Abstract PS01.11. 2020.

643 13. Baas P, Scherpereel A, Nowak AK, Fujimoto N, Peters S, Tsao AS, et al.
644 First-line nivolumab plus ipilimumab in unresectable malignant pleural
645 mesothelioma (CheckMate 743): a multicentre, randomised, open-label, phase 3
646 trial. Lancet. 2021;397(10272):375-86.

647 14. Bueno R, Stawiski EW, Goldstein LD, Durinck S, De Rienzo A, Modrusan
648 Z, et al. Comprehensive genomic analysis of malignant pleural mesothelioma
649 identifies recurrent mutations, gene fusions and splicing alterations. Nat Genet.
650 2016;48(4):407-16.

651 15. Hmeljak J, Sanchez-Vega F, Hoadley KA, Shih J, Stewart C, Heiman D,
652 et al. Integrative Molecular Characterization of Malignant Pleural Mesothelioma.
653 Cancer Discov. 2018;8(12):1548-65.

654 16. Björkqvist AM, Tammilehto L, Anttila S, Mattson K, Knuutila S. Recurrent
655 DNA copy number changes in 1q, 4q, 6q, 9p, 13q, 14q and 22q detected by
656 comparative genomic hybridization in malignant mesothelioma. Br J Cancer.
657 1997;75(4):523-7.

658 17. López-Ríos F, Chuai S, Flores R, Shimizu S, Ohno T, Wakahara K, et al.
659 Global gene expression profiling of pleural mesotheliomas: overexpression of
660 aurora kinases and P16/CDKN2A deletion as prognostic factors and critical
661 evaluation of microarray-based prognostic prediction. Cancer Res.
662 2006;66(6):2970-9.

18. Dacic S, Kothmaier H, Land S, Shuai Y, Halbwedl I, Morbini P, et al. Prognostic significance of p16/cdkn2a loss in pleural malignant mesotheliomas. Virchows Arch. 2008;453(6):627-35.

19. Hylebos M, Van Camp G, van Meerbeeck JP, Op de Beeck K. The Genetic Landscape of Malignant Pleural Mesothelioma: Results from Massively Parallel Sequencing. J Thorac Oncol. 2016;11(10):1615-26.

20. Frizelle SP, Grim J, Zhou J, Gupta P, Curiel DT, Geradts J, et al. Re-expression of p16INK4a in mesothelioma cells results in cell cycle arrest, cell death, tumor suppression and tumor regression. Oncogene. 1998;16(24):3087-95.

21. Middleton G, Fletcher P, Popat S, Savage J, Summers Y, Greystoke A, et al. The National Lung Matrix Trial of personalized therapy in lung cancer. Nature. 2020;583(7818):807-12.

22. Sherr CJ, Beach D, Shapiro GI. Targeting CDK4 and CDK6: From Discovery to Therapy. Cancer Discov. 2016;6(4):353-67.

23. Finn RS, Crown JP, Lang I, Boer K, Bondarenko IM, Kulyk SO, et al. The cyclin-dependent kinase 4/6 inhibitor palbociclib in combination with letrozole versus letrozole alone as first-line treatment of oestrogen receptor-positive, HER2-negative, advanced breast cancer (PALOMA-1/TRIO-18): a randomised phase 2 study. Lancet Oncol. 2015;16(1):25-35.

24. Turner NC, Huang Bartlett C, Cristofanilli M. Palbociclib in Hormone-Receptor-Positive Advanced Breast Cancer. N Engl J Med. 2015;373(17):1672-3.

25. Oie HK, Russell EK, Carney DN, Gazdar AF. Cell culture methods for the establishment of the NCI series of lung cancer cell lines. J Cell Biochem Suppl. 1996;24:24-31.

26. Nadal E, Chen G, Gallegos M, Lin L, Ferrer-Torres D, Truini A, et al. Epigenetic inactivation of microRNA-34b/c predicts poor disease-free survival in early-stage lung adenocarcinoma. Clin Cancer Res. 2013;19(24):6842-52.

692 27. Bollard J, Miguela V, Ruiz de Galarreta M, Venkatesh A, Bian CB, Roberto
693 MP, et al. Palbociclib (PD-0332991), a selective CDK4/6 inhibitor, restricts tumour
694 growth in preclinical models of hepatocellular carcinoma. Gut. 2017;66(7):1286-
695 96.

696 28. Püschel F, Muñoz-Pinedo C. Measuring the Activation of Cell Death
697 Pathways upon Inhibition of Metabolism. Methods Mol Biol. 2019;1862:163-72.

698 29. Bonelli MA, Digiacomo G, Fumarola C, Alfieri R, Quaini F, Falco A, et al.
699 Combined Inhibition of CDK4/6 and PI3K/AKT/mTOR Pathways Induces a
700 Synergistic Anti-Tumor Effect in Malignant Pleural Mesothelioma Cells.
701 Neoplasia. 2017;19(8):637-48.

702 30. Core Team. R: A language and environment for statistical computing. R
703 Foundation for Statistical Computing, Vienna, Austria. . 2020.

704 31. Ambrogio C, Carmona FJ, Vidal A, Falcone M, Nieto P, Romero OA, et al.
705 Modeling lung cancer evolution and preclinical response by orthotopic mouse
706 allografts. Cancer Res. 2014;74(21):5978-88.

707 32. Campisi J, d'Adda di Fagagna F. Cellular senescence: when bad things
708 happen to good cells. Nat Rev Mol Cell Biol. 2007;8(9):729-40.

709 33. Finn RS, Dering J, Conklin D, Kalous O, Cohen DJ, Desai AJ, et al. PD
710 0332991, a selective cyclin D kinase 4/6 inhibitor, preferentially inhibits
711 proliferation of luminal estrogen receptor-positive human breast cancer cell lines
712 in vitro. Breast Cancer Res. 2009;11(5):R77.

713 34. Goel S, DeCristo MJ, Watt AC, BrinJones H, Sceneay J, Li BB, et al.
714 CDK4/6 inhibition triggers anti-tumour immunity. Nature. 2017;548(7668):471-5.

715 35. Salvador-Barbero B, Alvarez-Fernández M, Zapatero-Solana E, El Bakkali
716 A, Menéndez MDC, López-Casas PP, et al. CDK4/6 Inhibitors Impair Recovery
717 from Cytotoxic Chemotherapy in Pancreatic Adenocarcinoma. Cancer Cell.
718 2020;38(4):584.

719 36. Ruscetti M, Leibold J, Bott MJ, Fennell M, Kulick A, Salgado NR, et al. NK
720 cell-mediated cytotoxicity contributes to tumor control by a cytostatic drug

combination. Science. 2018;362(6421):1416-22.

37. Wagner V, Gil J. Senescence as a therapeutically relevant response to CDK4/6 inhibitors. Oncogene. 2020;39(29):5165-76.

38. Bezzi M, Teo SX, Muller J, Mok WC, Sahu SK, Vardy LA, et al. Regulation of constitutive and alternative splicing by PRMT5 reveals a role for Mdm4 pre-mRNA in sensing defects in the spliceosomal machinery. Genes Dev. 2013;27(17):1903-16.

39. AbuHammad S, Cullinane C, Martin C, Bacolas Z, Ward T, Chen H, et al. Regulation of PRMT5-MDM4 axis is critical in the response to CDK4/6 inhibitors in melanoma. Proc Natl Acad Sci U S A. 2019;116(36):17990-8000.

40. Varin E, Denoyelle C, Brotin E, Meryet-Figuière M, Giffard F, Abeilard E, et al. Downregulation of Bcl-xL and Mcl-1 is sufficient to induce cell death in mesothelioma cells highly refractory to conventional chemotherapy. Carcinogenesis. 2010;31(6):984-93.

Figure legends

Figure 1. Quantification of the expression levels of key cell cycle regulators and response to treatment with CDK4/6 inhibitors in a panel of commercial MPM cell lines (MSTO-211H, H28, H226, H2052, H2452) and primary patient-derived cultures (ICO_MPM1, ICO_MPM2, ICO_MPM3). *(A)* Baseline protein expression levels by Western blot of CDK4, CDK6, cyclin D1, Rb, phosphor-RB and p16. *(B)* Number of viable cells was determined *in vitro* by cell counting in the panel of cells after three days of treatment with increasing concentrations (0, 10, 100, 500 nM) of abemaciclib or palbociclib. Bar plots represent the means ± SD of 3 measurements in 3 biological replicates. Adjusted p-values were calculated with Wilcoxon signed rank tests. In the graph, the p values are reported with respected to 0 nM (*p < 0.05; **p < 0.01). (*C*) Colony formation assay displaying treatment response to abemaciclib and palbociclib. A representative image from 3 biological independent replicates is displayed.

Figure 2. Effects of cell line treatments with CDK4/6 inhibitors abemaciclib or palbociclib at 0, 250 or 500 nM doses to induce *(A and B)* cell-cycle arrest and (*C*) senescence. (*A*) MSTO-211H, H28 and ICO_MPM3 cells were untreated and treated with both inhibitors for 24 hours and DNA content analysed by flow cytometry. Cell cycle arrest at G1 phase was induced by both CDK4/6 inhibitors in the cell lines. (*B*) Percentage of cells in each phase of the cell cycle phase in response to abemaciclib and palbociclib treatments at doses of 0, 250 or 500 nM for 24 hours. Cell cycle phase distribution analysis was done using FlowJo software. Each value represents the mean ± SD of 3 replicates. Adjusted p values were considered significant when mean differed from control within each phase of the cell cycle (*p < 0.05; ***p < 0.001). (*C*) A significant increase in the number of SA-β-Gal positive cells was detected in MSTO-211H, H28 and ICO_MPM2 treated. Data are expressed as a percentage of senescent cells obtained from the mean value ± SD of 3 replicates. Adjusted p-values < 0.05 were considered significant.

Figure 3. *In vivo* treatment with palbociclib in MSTO-211H subcutaneous xenografted MPM model. A xenografted subcutaneous tumour model was established by inoculation of MSTO-211H cells into the flanks of athymic nude mice (n=7 per group). Tumours' volume (*A*) was monitored by calliper measure every four days (at each time point, a SD bar is shown). *(B)* Differences in tumour volume for each day were represented using boxplots and compared using Kruskal-Wallis test, adjusted by FDR and were significantly different at day 16. At the end of the experiment, mice were sacrificed and *(C* and *D)* the tumours were removed, weighted and photographed. Asterisks indicated absence of apparent macroscopic tumour at sacrifice, while residual cells were identified by H&E analysis. *(E)* Summary of the body weight values among first and last day of treatment from all mice in *in vivo* subcutaneous tumour xenograft growth experiment. Palbociclib did not exert any substantial change in the mice body weight. Differences were evaluated by Mann-Whitney test and adjusted for FDR. (F) Representative IHC images for (F.A) mouse macrophages that express F4/80 (brown staining) and (F.B) mouse NK cells that express NCR1 (brown staining) infiltrated in the subcutaneous MPM tumours xenografted in athymic nude mice after 26 days of treatment with vehicle, platinum plus pemetrexed or palbociclib. Inset photos contains the digital whole slide image showing the infiltrated area of tumour. Scale bar = 50 µm. Dot plots showing (*G*) the mean $F4/80^{+}$ intensity per pixel (x-axis) or *(J)* the percentage of $NCR1^{+}$ cells over total cells infiltrated in the subcutaneous MPM tumour xenegrafted in athymic nude mice after 26 days of treatment with vehicle, platinum plus pemetrexed or palbocilib (n= 5-7 per group). Data are expressed as single data values (dots) + the mean. ANOVA test was used to detect statistical differences between treatments ($*p < 0.05$).

Figure 4. In vivo treatment with CDK4/6 inhibitors in advanced orthotopic MPM models. Two advanced orthotopic models were generated by implantation in the lung of mice small solid fragments (2-3 mm^3) of previously generated (*A, B* and *C*) MSTO-211H subcutaneous cisplatin plus pemetrexed resistant tumour xenograft or (*D, E* and *F*) chemoresistant patient-derived tumour xenograft. (*A*) Kaplan-Meier curves showing survival of MSTO-211H orthotopic tumour-bearing mice (n=33). (*B*) Representative MSTO-211H images of orthotopic tumours

dissected from each group of treatment and (*C*) histological characterization on H&E sections (Scale bars = 100 µm). (D) Kaplan-Meier curves showing survival of ICO_MPM3 orthotopic tumour-bearing mice (n=29). (*E*) Representative images of patient-derived orthotopic tumours dissected from each group of treatment and (*F*) histological characterization on H&E sections (Scale bars = 100 µm). Both orthotopic models accurately reproduce human MPM disease characteristics as tumour grown from the site of implantation to all the pleural space. Tumour mass area is delimited by white line.

Figure 5. Kaplan-Meier plots of overall survival (OS) in MPM patients according to *(A) CDK4* and *(B) CDK6* gene expression levels based on data obtained from Bueno et al. (left column) and Hmeljak et al. (middle column) cohorts or the combination of both (right column). High levels of *CDK4* or *CDK6* (red line) were significantly associated with poor OS in patients with MPM. In each cohort, the high and low expression levels were defined based upon the median. P-values and hazard ratios (HR) were calculated by likelihood ratio test and multivariate Cox regression analysis respectively.

Acknowledgements

We thank CERCA Program / Generalitat de Catalunya for their institutional support and grant 2017SGR448. E.Nadal received support from the SLT006/17/00127 grant, funded by the Department of Health of the Generalitat de Catalunya by the call “Acció instrumental d’intensificació de professionals de la salut”.

Authors’ contributions

EA: Conceptualization, Methodology, Validation, Formal analysis, Investigation, Resources, Data Curation, Writing – Original Draft, Writing – Review & Editing, Visualization **AA:** Conceptualization, Software, Validation, Formal analysis, Resources, Data Curation, Writing – Review & Editing, Visualization **MMI**: Methodology, Investigation, Resources, Data curation **MHM:** Methodology, Validation, Investigation, Data Curation **DC:** Conceptualization, Software,

Validation, Formal analysis, Data Curation **MG:** Conceptualization, Resources, Writing – Review & Editing **EP:** Resources, Writing – Review & Editing **MS:** Resources, Writing – Review & Editing **SB:** Software, Validation, Data Curation **AJS:** Resources, Writing – Review & Editing **AD:** Resources, Writing – Review & Editing **RP:** Resources, Data Curation, Writing – Review & Editing **SP:** Resources, Writing – Review & Editing **SA:** Resources, Writing – Review & Editing **IE:** Resources, Writing – Review & Editing **RR:** Resources, Writing – Review & Editing **RL:** Resources, Validation, Data Curation **AV:** Resources, Validation, Data Curation **ED:** Data Curation **MV:** Resources, Validation, Data Curation **MSC:** Resources, Writing – Review & Editing **DF:** Resources, Validation, Formal analysis, Investigation, Data Curation, Writing – Review & Editing **CMP:** Conceptualization, Methodology, Validation, Formal analysis, Investigation, Data Curation, Writing – Review & Editing, Visualization **AV:** Conceptualization, Methodology, Validation, Formal analysis, Investigation, Data Curation, Writing – Review & Editing, Visualization **XS:** Conceptualization, Software, Formal analysis, Data Curation, Writing – Review & Editing, Visualization **EN:** Conceptualization, Methodology, Validation, Formal analysis, Investigation, Resources, Data Curation, Writing – Original Draft, Writing – Review & Editing, Visualization, Supervision, Project administration, Funding acquisition.

Ethics approval and consent to participate

The retrospective cohort was approved by a National Ethical Committee, under the references 4/LO/1527 (a translational research platform entitled *Predicting Drug and Radiation Sensitivity in Thoracic Cancers – also approved by University Hospitals of Leicester NHS Trust under the reference IRAS131283*) and 14/EM/1159 (retrospective cohort). Pleural effusions samples were obtained after patients signed the informed consent approved by the Hospital de Bellvitge Ethical Committee (PR152/14). All the animal experiments were performed in accordance with protocols approved by Animal Research Ethics Committee at IDIBELL. This study was performed in accordance with the principles outlined in the Declaration of Helsinki.

Data availability

All data generated or analysed during this study will be stored in EGA and available on reasonable request.

Funding information

This study was supported by grants from Instituto de Salud Carlos III (Grants PI14/01109 and PI18/00920) (Co-funded by European Regional Development Fund. ERDF, a way to build Europe), Spanish Society of Medical Oncology grant for emerging research groups and from Pfizer (WI244174) to Ernest Nadal. M.H-M was supported by a Marie Skłodowska-Curie grant, agreement No 766214.

898 **Figures and Tables**

899

Figure 1

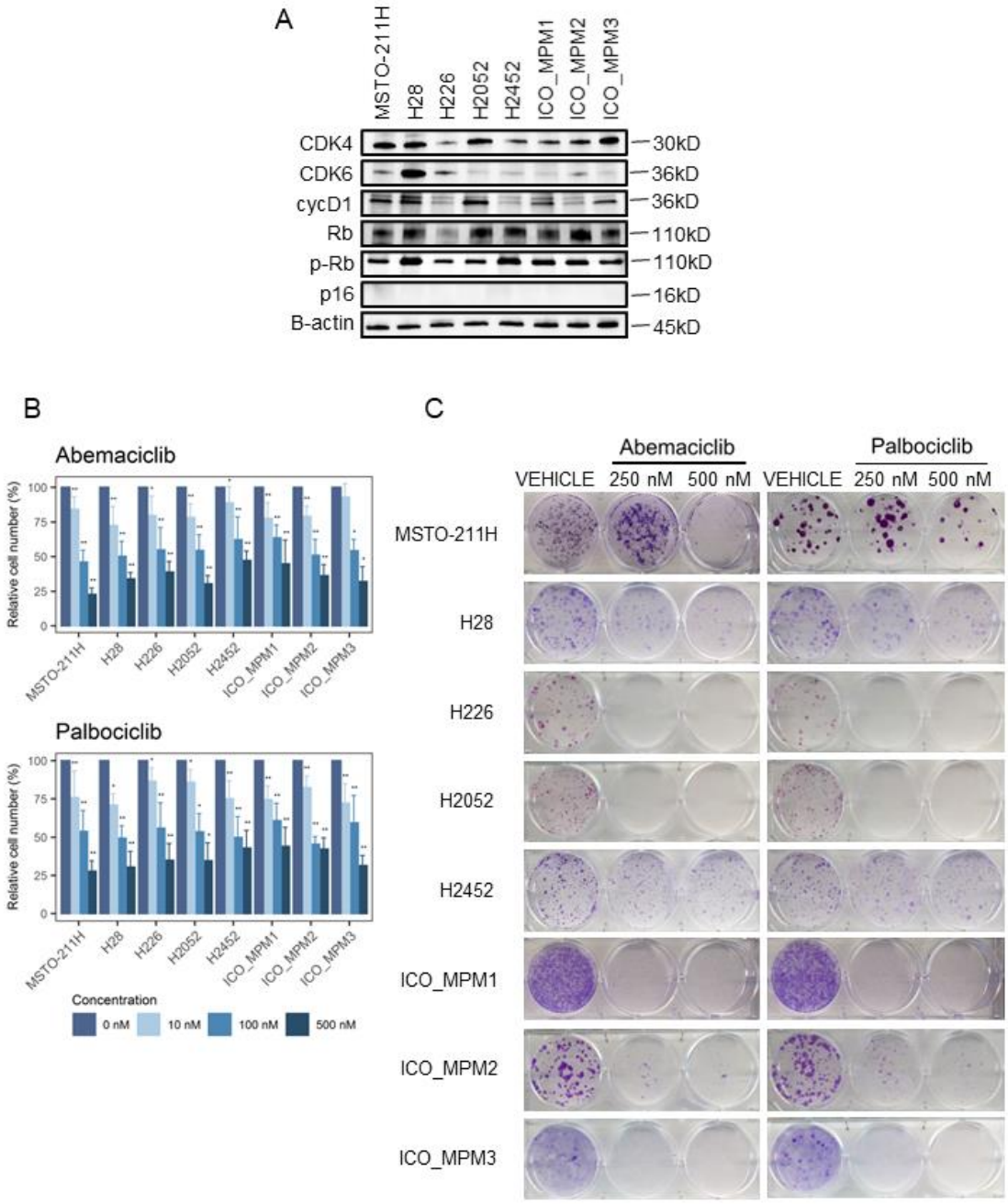

900

Figure 2

A

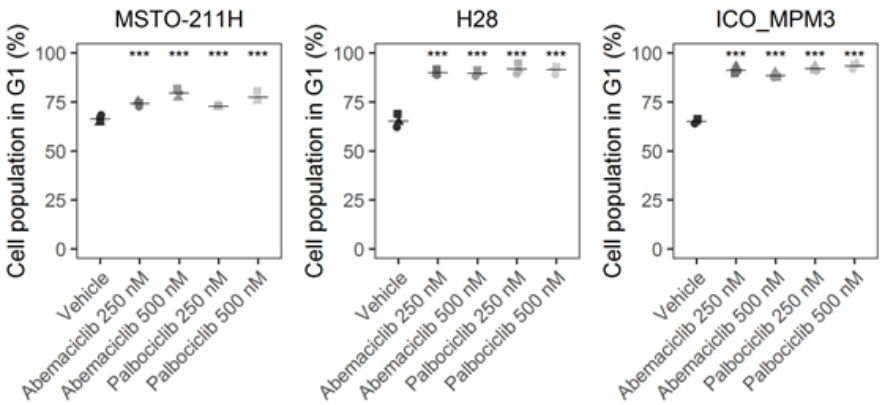

B

MPM cell line	Treatment	% of cells at G1	% of cells at G2	% of cells at S	% of cells at subG1
MSTO-211H	Vehicle	66.25 ± 1.89	18.56 ± 2.86	11.11 ± 0.91	1.38 ± 0.51
	Abemaciclib 250 nM	74.14 ± 1.37 ***	12.72 ± 0.72 ***	9.36 ± 1.72 ***	2.13± 0.70 ***
	Abemaciclib 500 nM	79.54 ± 2.25 ***	8.67 ± 1.09 ***	7.34 ± 1.21 ***	3.22 ± 0.95 ***
	Palbociclib 250 nM	72.86 ± 0.34 ***	13.75 ± 0.31 ***	9.45 ± 0.35 ***	2.15 ± 0.26 ***
	Palbociclib 500 nM	77.40 ± 2.70 ***	11.12 ± 1.15 ***	8.11 ± 0.63 ***	1.81 ± 0.44 ***
H28	Vehicle	65.23 ± 3.37	18.40 ± 1.50	11.29 ± 1.43	3.37 ± 2.67
	Abemaciclib 250 nM	89.96 ± 1.48 ***	5.66 ± 0.32 ***	1.97 ± 0.47 ***	1.75 ± 0.70 ***
	Abemaciclib 500 nM	89.69 ± 1.50 ***	6.59 ± 0.55 ***	1.46 ± 0.38 ***	1.70 ± 0.26 ***
	Palbociclib 250 nM	91.81 ± 2.64 ***	4.59 ± 0.57 ***	1.53 ± 0.87 ***	1.33 ± 1.44 ***
	Palbociclib 500 nM	91.42 ± 2.10 ***	4.70 ± 0.63 ***	1.79 ± 0.64 ***	1.71 ± 0.42 ***
ICO_MPM3	Vehicle	65.11 ± 1.12	22.19 ± 0.33	8.72 ± 1.06	0.91 ± 0.27
	Abemaciclib 250 nM	91.14 ± 1.88 ***	5.71 ± 1.79 ***	1.29 ± 0.17 ***	0.98 ± 0.17
	Abemaciclib 500 nM	88.40 ± 1.45 ***	8.22 ± 1.70 ***	1.21 ± 0.17 ***	0.84 ± 0.41
	Palbociclib 250 nM	91.89 ± 1.20 ***	4.70 ± 1.17 ***	1.60 ± 0.71 ***	1.08 ± 0.81 *
	Palbociclib 500 nM	93.39 ± 1.47 ***	4.00 ± 1.05 ***	0.98 ± 0.10 ***	0.87 ± 0.47

C

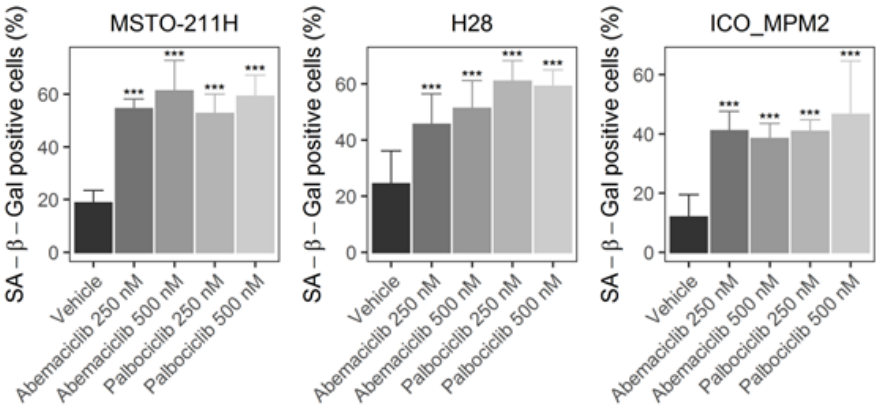

Figure 3

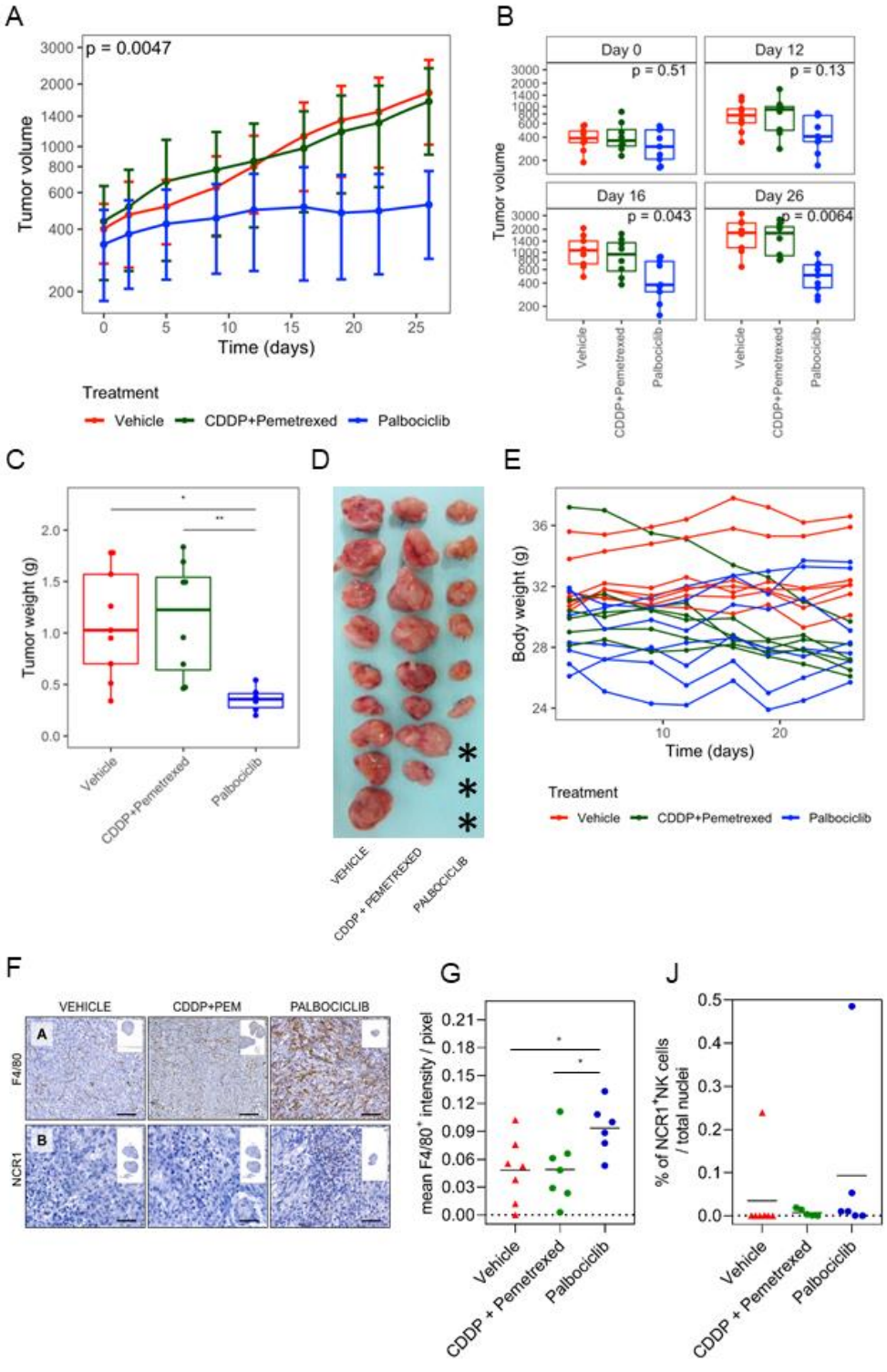
A
p = 0.0047
Tumor volume
Time (days)
Treatment
Vehicle
CDDP+Pemetrexed
Palbociclib
B
Day 0
p = 0.51
Day 12
p = 0.13
Day 16
p = 0.043
Day 26
p = 0.0064
Tumor volume
Vehicle
CDDP+Pemetrexed
Palbociclib
C
Tumor weight (g)
D
VEHICLE
CDDP + PEMETREXED
PALBOCICLIB
E
Body weight (g)
Time (days)
Treatment
Vehicle
CDDP+Pemetrexed
Palbociclib
F
VEHICLE
CDDP+PEM
PALBOCICLIB
F4/80
NCR1
G
mean F4/80+ intensity / pixel
Vehicle
CDDP + Pemetrexed
Palbociclib
J
% of NCR1+NK cells / total nuclei
Vehicle
CDDP + Pemetrexed
Palbociclib

Figure 4

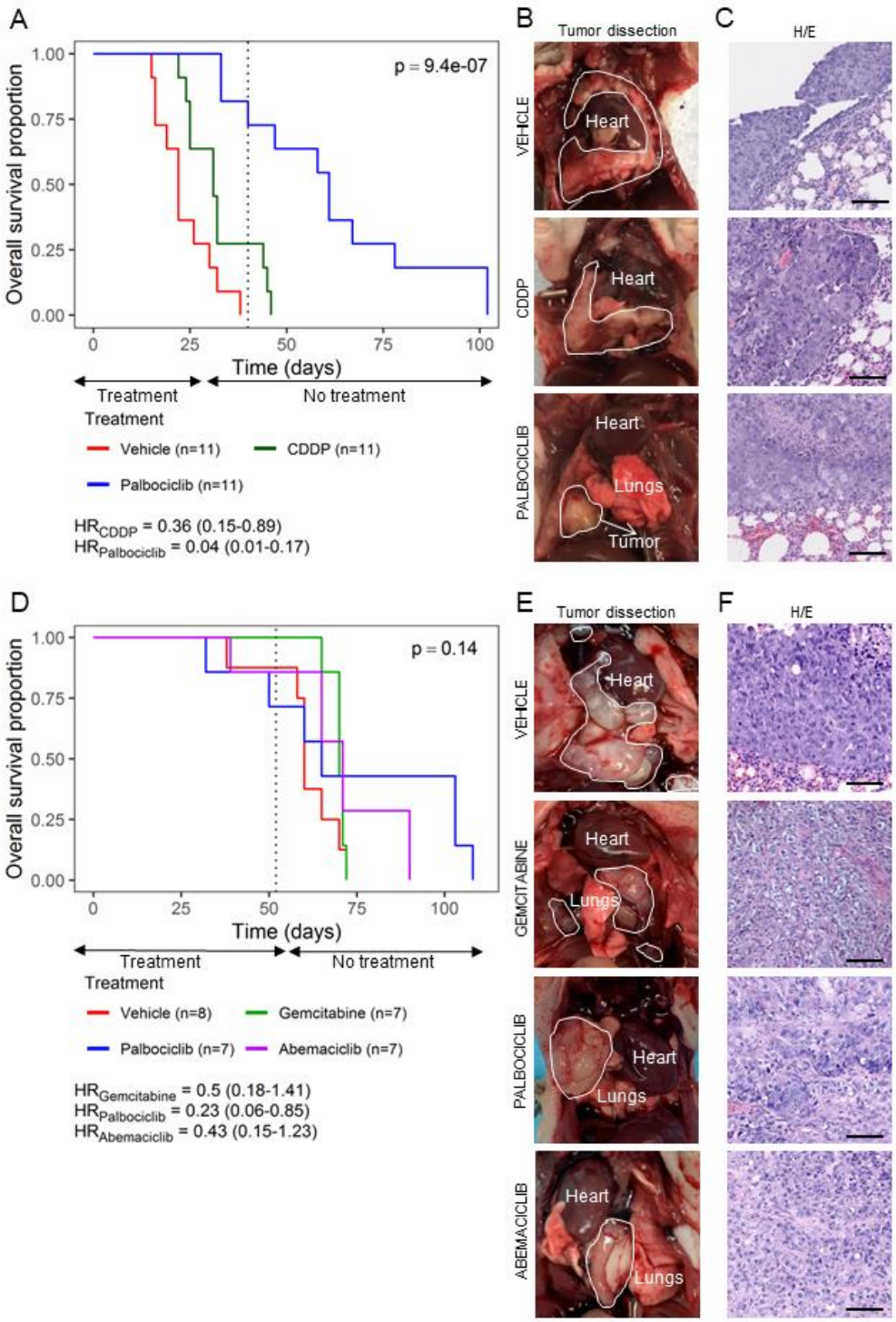
A
Overall survival proportion
1.00
0.75
0.50
0.25
0.00
p = 9.4e-07
0
25
50
75
100
Time (days)
Treatment
No treatment
Treatment
Vehicle (n=11)
CDDP (n=11)
Palbociclib (n=11)
HR$_{CDDP}$ = 0.36 (0.15-0.89)
HR$_{Palbociclib}$ = 0.04 (0.01-0.17)
B
Tumor dissection
C
H/E
VEHICLE
CDDP
PALBOCICLIB
Heart
Lungs
Tumor
D
Overall survival proportion
p = 0.14
Time (days)
Treatment
No treatment
Treatment
Vehicle (n=8)
Gemcitabine (n=7)
Palbociclib (n=7)
Abemaciclib (n=7)
HR$_{Gemcitabine}$ = 0.5 (0.18-1.41)
HR$_{Palbociclib}$ = 0.23 (0.06-0.85)
HR$_{Abemaciclib}$ = 0.43 (0.15-1.23)
E
Tumor dissection
F
H/E
VEHICLE
GEMCITABINE
PALBOCICLIB
ABEMACICLIB
Heart
Lungs

Figure 5

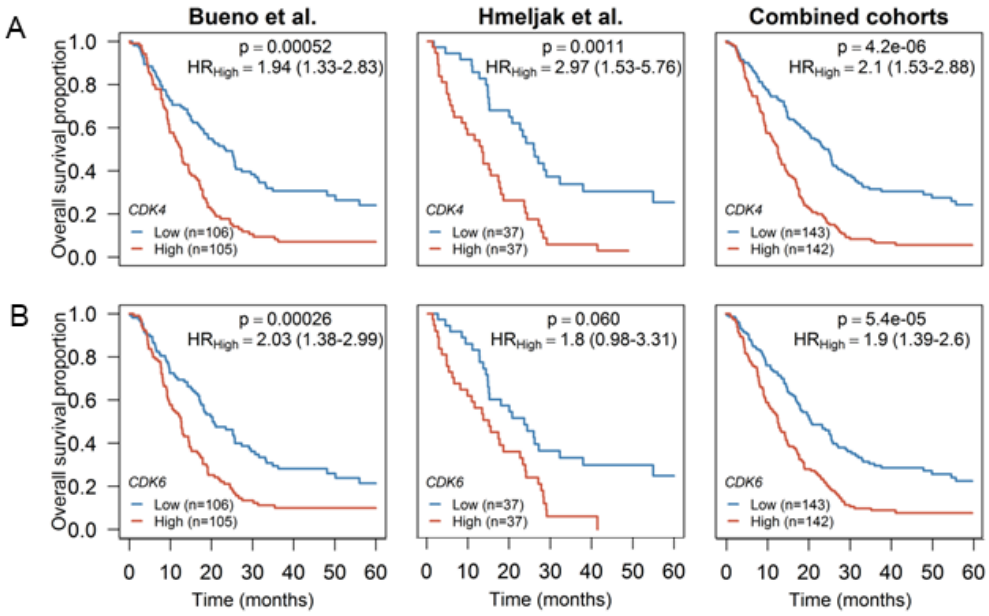

910

911

Table 1. Clinicopathological characteristics and main genomic and protein alterations found in primary cell lines were derived from patients with pleural malignant mesothelioma. Additional predicted driver mutations have been identified using Cancer Genome Interpreter. (WES: whole exome sequencing; FISH: fluorescence in situ hybridization).

	Clinicopathological features					**Molecular characterization by WES and FISH**				
ID	**Age**	**Sex**	**Asbestos exposure**	**Histology**	**Prior chemotherapy**	***BAP1* (WES)**	***TP53* (WES)**	***NF2* (WES)**	***CDKN2A* (FISH)**	**Additional predicted driver mutations**
ICO_MPM1	77	M	No	Epithelioid	Yes	p.(Lys651_Lys661 del)	p.(Asn92Cys*26)	WT	Hemizygous deletion	*DHX15* p.(Pro478His) *SF3B1* p.(Tyr623Cys)
ICO_MPM2	73	F	Yes	Epithelioid	No	p.(Arg60*)	WT	WT	Hemizygous deletion	*CSNK2A1* p.(Asp210Tyr)
ICO_MPM3	70	M	No	Epithelioid	Yes	WT	WT	WT	Homozygous deletion	*ACO1* p.(Arg802His) *ABL1* p.(Gly1060Asp) *INPP4A* p.(Arg244Trp) *EP300* p.(Arg1356*) *SPEN* p.(Ser260Ile) *CREBBP* p.(Trp1718*)